

Synthesis of FePt Nanocubes and Their Oriented Self-Assembly

Min Chen,^{†,§,⊥} Jaemin Kim,[‡] J. P. Liu,[#] Hongyou Fan,^{§,⊥} and Shouheng Sun^{*,†,‡}

IBM T. J. Watson Research Center, Yorktown Heights, New York 10598, Department of Physics, University of Texas, Arlington, Texas 76019, Advance Materials Laboratory, Sandia National Laboratories, Albuquerque, New Mexico 87106, UNM/NSF Center for Micro-Engineered Materials, University of New Mexico, Albuquerque, New Mexico 87131, and Department of Chemistry, Brown University, Providence, Rhode Island 02912

Received March 11, 2006; E-mail: ssun@brown.edu

Fabrication of ordered nanomagnet arrays with controlled magnetic alignment is an important goal in achieving high density information storage¹ and high performance permanent magnets.² For a uniaxial anisotropic nanomagnet, magnetic alignment infers that magnetization of the magnet lies only along the “easy direction”. In ferromagnetic hysteresis behaviors, such an alignment corresponds to a hysteresis loop with high squareness, which leads to the remanent magnetization value close to the saturation one. Magnets with this magnetic behavior can have distinct magnetization reversals and retain maximum magnetic energy for data storage and permanent magnetic applications. Among all available hard magnetic nanomaterials, face centered tetragonal (fct) structured FePt nanocrystals are especially interesting because they have uniaxial anisotropy along the [001] direction and their magnetocrystalline anisotropy constant, K , which measures the ease of magnetization reversal along the [001] direction, can reach as high as 10^7 J/m³,³ a value that is one of the largest among the known hard magnetic materials. Such hard magnetic FePt nanocrystals have been made by high temperature (250–300 °C) solution phase synthesis, followed by nanocrystal self-assembly and high temperature (usually >550 °C) thermal annealing.⁴ As synthesized, the FePt nanoparticles possess face centered cubic (fcc) structure and are superparamagnetic at room temperature. Thermal annealing converts the fcc FePt to fct FePt, yielding nanocrystalline magnets with coercivity reaching as high as 30 kOe.⁵ Despite these synthetic progresses, there is still no evidence that magnetic orientation in FePt nanocrystal arrays can be established unless a physical deposition process is used,⁶ which often has difficulty in controlling nanomagnet sizes and morphologies.

Here we report a chemical synthesis of FePt nanocubes and their self-assembly into FePt nanocrystal superlattice arrays with controlled texture and magnetic alignment. We recently reported that the shape of the MnFe₂O₄ nanoparticles could induce texture in self-assembled superlattice arrays.⁷ In an assembly containing cube-like nanoparticles, the array shows (100) texture, while in a polyhedron-like nanoparticle assembly, (110) texture was obtained. These early experiments indicate that structural alignment of each particle can be achieved if the shape of the nanoparticles is controlled. In searching for shape-controlled synthesis of FePt nanoparticles, we found that simultaneous decomposition of Fe(CO)₅ and reduction of Pt(acac)₂ without polyol as a reducing agent yielded FePt nanoparticles with sizes tunable from 3 to 9 nm.⁸ Our further synthetic studies revealed that, by controlling the addition sequence of the stabilizers (oleic acid and oleylamine) and Fe/Pt ratio in the precursors, FePt nanocubes could be prepared at

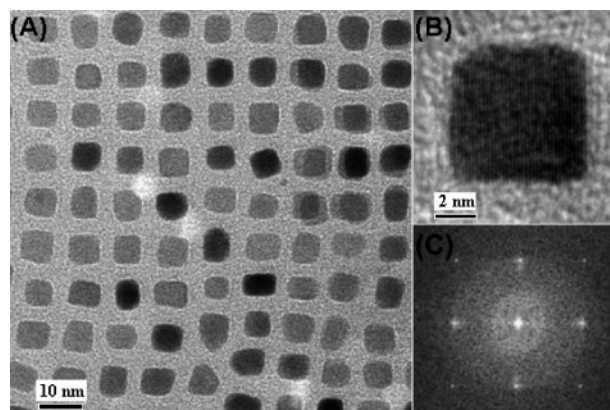


Figure 1. TEM bright field images of (A) 6.9 nm Fe₅₀Pt₅₀ nanocubes; (B) HRTEM of a single FePt nanocube; (C) FFT of the cube in (B).

relatively low temperature (205 °C). This communication describes the synthesis of FePt nanocubes and self-assembly of these cubes into textured superlattice arrays. The work demonstrates that shape-controlled synthesis and self-assembly can offer a simple solution to fabrication of magnetically aligned FePt nanocrystal arrays that are promising for single nanoparticle recording and for high performance exchange-spring nanocomposite magnet applications.

The 6.9 nm Fe₅₀Pt₅₀ nanocubes were synthesized by mixing oleic acid and Fe(CO)₅ with benzyl ether/octadecene solution of Pt(acac)₂ and heating the mixture to 120 °C for about 5 min before oleylamine was added, and the mixture was heated at 205 °C for 2 h.⁹ The key to the success of the nanocube synthesis at 205 °C, rather than 300 °C—the temperature normally used for FePt nanoparticle synthesis—is that more Fe(CO)₅ should be introduced to the reaction system. The shape is controlled by adding oleic acid first during the reaction. The nanocubes are likely formed from the growth of the cubic Pt-rich nuclei generated during the initial stage of the reaction, as the –COOH does not have a strong tendency to bind to Pt. It is known that the surface energy of crystallographic planes of a fcc Pt crystal generally follow the trend of (111) < (100).¹⁰ In a kinetic growth process, the Fe-rich species prefer to deposit on the (100) plane, leading to the formation of a cube. If oleylamine was added first, sphere-like FePt nanoparticles were separated. This indicates that the amine reacts with Pt, forming a stable Pt–NH₂– complex and hindering the nucleation process. The resulting nuclei may contain more Fe in this case, producing an amorphous spherical structure. The uniform FePt nanocubes or spherical FePt nanoparticles must be derived from atomic diffusion between a Pt-rich core and an Fe-rich shell in a process that is similar to what has been described in a previous publication.⁸

Transmission electron microscopic (TEM) image of the 6.9 nm Fe₅₀Pt₅₀ nanocubes is given in Figure 1A. Figure 1B is the high-resolution TEM (HRTEM) image of a single Fe₅₀Pt₅₀ nanocube.

[†] IBM T. J. Watson Research Center.

[#] University of Texas at Arlington.

[§] Sandia National Laboratories.

[⊥] University of New Mexico.

[‡] Brown University.

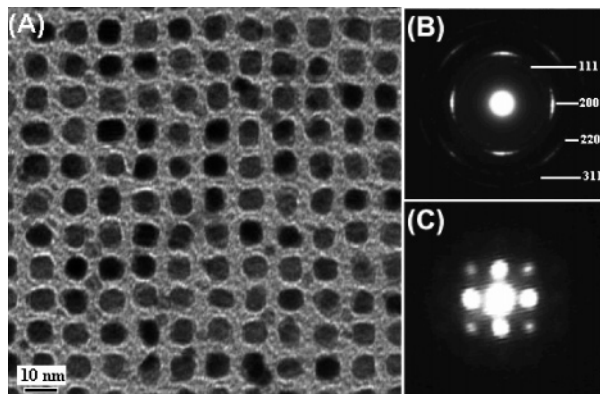


Figure 2. (A) TEM image of a multilayer assembly of 6.9 nm Fe₅₀Pt₅₀ nanocubes; and (B) SAED of the assembly in (A), and (C) small angle diffraction of the assembly in (A).

It shows the lattice fringes with an inter-fringe distance of 0.192 nm, close to the lattice spacing of the {100} planes at 0.1908 nm in the fcc structured FePt. Fast Fourier transformation (FFT) of the single particle (Figure 1C) reveals a 4-fold symmetry, consistent with the fcc structure projected from the [001] direction. These indicate that the {100} lattice fringes are parallel to the edges of the cube.

Controlled evaporation of the carrier solvent from the hexane dispersion (~2 mg/mL) of the nanocubes led to a Fe₅₀Pt₅₀ nanocube superlattice array, as shown in Figure 2. FFT of the image reveals that the assembly has the cubic packing with a view from the [001] direction showing a 4-fold symmetry.⁹ The image from a 40° tilting angle shows that the bottom layer of the FePt nanocube array is lined with the top layer.⁹ This assembly pattern is energetically favored as it gives the maximum van der Waals interaction energy arising from face–face interactions in short distance of the cube assembly.¹¹ The interparticle distance is around 4–5 nm, close the simple thickness addition of the cube coating layer (2–2.5 nm, the length of oleate or oleylamine).

Selected area electron diffraction (SAED) of the assembly in Figure 2A exhibits four bright (200) spots that are linked by a 4-fold symmetry, as shown in Figure 2B. The (111) diffraction ring is very weak in this diffraction pattern. These indicate that the assembly in Figure 2A is (100) textured. The textured cubic assembly is further revealed by a small angle diffraction of the assembly (Figure 2C). X-ray diffraction (XRD) of the self-assembled FePt nanocubes on a Si(100) substrate also shows a strong (200) reflection (Figure S1B). This is markedly different from that of a 3D randomly oriented FePt nanoparticle assembly with a strong (111) peak,⁸ indicating that each nanocube in the assembly has a preferred crystal orientation with {100} planes parallel to the substrate.

Thermal annealing of the FePt nanocube superlattice induces FePt structure transformation from fcc to fct. The XRD pattern of the annealed assembly (675 °C under Ar for 1 h) has two strong (001) and (200) peaks, as shown in Figure 3A. The narrowed peaks indicate the particle growth during the annealing process. However, the peak intensity is different from that of the spherical FePt nanoparticle assembly, which shows only one strong (111) peak.⁸ This indicates that (001) and (200) planes in the thermally annealed FePt nanocube array are now parallel and perpendicular to the substrate. Figure 3B is the room temperature hysteresis loop of the annealed FePt nanocube assembly with coercivity at 22 kOe. The loop is exactly the same in both parallel and perpendicular directions of the assembly, confirming what is concluded from the XRD

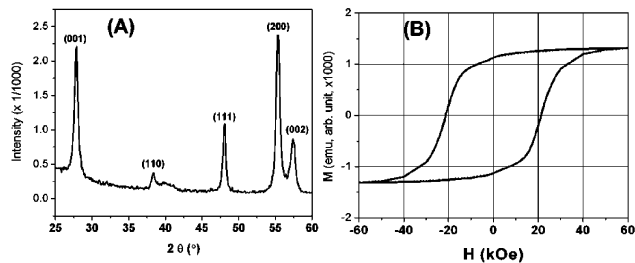


Figure 3. (A) XRD of thermally annealed FePt nanocube assembly on a Si surface, and (B) room temperature in-plane hysteresis loop of the FePt nanocube assembly in (A).

analysis in Figure 3A. Detailed study in shape-controlled magnetic alignment is underway.

In conclusion, we have reported that FePt nanocubes can be produced at 205 °C by controlling Fe/Pt ratio in the precursors and addition sequence of oleic acid and oleylamine. Self-assembly of these FePt nanocubes creates a (100) textured array. Thermal annealing induces the internal particle structure change and transforms the nanocube assembly from superparamagnetic to ferromagnetic. The work demonstrates that it is possible to use particle shape to control assembly texture and further on magnetic alignment. When this is achieved, shape-controlled synthesis and self-assembly will evolve as a convenient approach to magnetically aligned FePt nanocrystal arrays for single particle recording and for maximization of energy product in an exchange-spring nanocomposite system.

Acknowledgment. The work was supported by U.S. DOD/DARPA under Grant No. DAAD19-03-1-0038, ONR/MURI under Grant N00014-05-1-0497, and DOE Basic Energy Sciences Program under contract DE-AC04-94AL85000.

Supporting Information Available: Experimental procedures and characterization data of the FePt assembly. This material is available free of charge via the Internet at <http://pubs.acs.org>.

References

- (1) (a) Weller, D.; Moser, A. *IEEE Trans. Magn.* **1999**, *35*, 4423–4439. (b) Weller, D.; Doerner, M. E. *Annu. Rev. Mater. Sci.* **2000**, *30*, 611–644. (c) Moser, A.; Takano, K.; Margulies, D. T.; Albrecht, M.; Sonobe, Y.; Ikeda, Y.; Sun, S.; Fullerton, E. E. *J. Phys. D: Appl. Phys.* **2002**, *35*, R157–R167.
- (2) (a) Kneller, E. F.; Hawig, R. *IEEE Trans. Magn.* **1991**, *27*, 3588–3600. (b) Skomski, R.; Coey, J. M. D. *Phys. Rev. B* **1993**, *48*, 15812–15816. (c) Schrefl, T.; Kronmüller, H.; Fidler, J. *J. Magn. Magn. Mater.* **1993**, *127*, L273–L277. (d) Zeng, H.; Li, J.; Wang, Z. L.; Liu, J. P.; Sun, S. *Nature* **2002**, *420*, 395–398.
- (3) Farrow, R. F. C.; Weller, D.; Marks, R. F.; Toney, M. F.; Cebollada, A.; Harp, G. R. *J. Appl. Phys.* **1996**, *79*, 5967–5969.
- (4) (a) Sun, S.; Murray, C. B.; Weller, D.; Folks, L.; Moser, A. *Science* **2000**, *287*, 1989–1992. (b) Sun, S.; Fullerton, E. E.; Weller, D.; Murray, C. B. *IEEE Trans. Magn.* **2001**, *37*, 1239–1243. (c) Sun, S. *Adv. Mater.* **2006**, *18*, 393–403.
- (5) Elkins, K.; Li, D.; Poudyal, N.; Nandwana, V.; Jin, Z.; Chen, K.; Liu, J. P. *J. Phys. D: Appl. Phys.* **2005**, *38*, 2306–2309.
- (6) (a) Thiele, J. U.; Folks, L.; Toney, M. F.; Weller, D. K. *J. Appl. Phys.* **1998**, *84*, 5686–5692. (b) Bian, B.; Sato, K.; Hirotsu, Y.; Makino, A. *Appl. Phys. Lett.* **1999**, *75*, 3686–3688. (c) Kang, K.; Zhang, Z. G.; Papusoi, C.; Suzuki, T. *Appl. Phys. Lett.* **2003**, *82*, 3284–3286. (d) Shima, T.; Takahashi, K.; Takahashi, Y. K.; Hono, K. *Appl. Phys. Lett.* **2004**, *85*, 2571–2573. (e) Shen, W. K.; Judy, J. H.; Wang, J. P. *J. Appl. Phys.* **2005**, *97*, 10H301/1–10H301/3.
- (7) Zeng, H.; Rice, P. M.; Wang, S. X.; Sun, S. *J. Am. Chem. Soc.* **2004**, *126*, 11458–11459.
- (8) Chen, M.; Liu, J. P.; Sun, S. *J. Am. Chem. Soc.* **2004**, *126*, 8394–8395.
- (9) See Supporting Information.
- (10) Wang, Z. L. *J. Phys. Chem. B* **2000**, *104*, 1153–1175.
- (11) (a) Korgel, B. A.; Fullam, S.; Connolly, S.; Fitzmaurice, D. *J. Phys. Chem. B* **1998**, *102*, 8379–8388. (b) Yamamuro, S.; Sumiyama, K. *Chem. Phys. Lett.* **2006**, *418*, 166–169.

JA061704X